Desalination and Water Treatment
www.deswater.com

doi: 10.5004/dwt.2017.0196

62 (2017) 346–354
February

Removal of Cadmium (II) from aqueous solution by zinc oxide nanoparticles: kinetic and thermodynamic studies

L. Khezami[a], Kamal K. Taha[a,b,*], Ezzeddine Amami[c], Imed Ghiloufi[d,e], Lassaad El Mir[d,e]

[a]*Department of Chemistry, College of Sciences, Al Imam Mohammad Ibn Saud Islamic University (IMSIU), Riyadh 11432, Saudi Arabia, Tel. +966565205871; email: lkhezami@gmail.com (L. Khezami); Tel. +966551799861; email: kamaltha60@gmail.com (K.K. Taha)*
[b]*College of Applied and Industrial Sciences, University of Bahri, Khartoum, Sudan*
[c]*University Tunis El Manar. Research Unit "Materials Chemistry and the Environment"Higher Institute of Applied Biological Sciences of Tunis (ISSBAT) 9. street Zouhair Essafi Tunis in 1006, Tel. +21626433736; email: ezzeddineamami@yahoo.fr*
[d]*Department of Physics, College of Sciences, Al Imam Mohammad Ibn Saud Islamic University (IMSIU), Riyadh 11432, Saudi Arabia, Tel. +966112582174; email: ghiloufimed@yahoo.fr (I. Ghiloufi); Tel. +96653144830; email: Lassaad.Elmir@fsg.rnu.tn (L. El Mir)*
[e]*Laboratory of Physics of Materials and Nanomaterials Applied at Environment (LaPhyMNE), Faculty of Sciences, GabesUniversity, Gabes, Tunisia*

Received 16 February 2016; Accepted 25 July 2016

ABSTRACT

In this study, the removal of cadmium ions by ZnO nanoparticles, prepared by a modified sol-gel method, was investigated. The kinetics, thermodynamic and equilibrium parameters of the cadmium ion adsorption on the nanomaterial were determined in batch mode experiments. The adsorption process was found to be highly concentration dependent, and the adsorption rate increased proportionally with temperature indicating an endothermic process. The kinetics of the adsorption process was found to follow the pseudo-second-order rate law. The adsorption isotherm data were in good agreement with the Langmuir model. The maximum adsorption capacity of ZnO nanoparticles for Cd(II) was found to be 217.4 mg.g^{-1} at 328 K. Thermodynamic parameters revealed the endothermic and spontaneous nature of the adsorption process. Nevertheless, the global reaction rate is probably controlled by the intra-particular diffusion of Cd(II) ions.

Keywords: ZnO nanoparticles; Cadmium removal; Adsorption kinetic and equilibrium

1. Introduction

Hazards and risks to which living organisms and ecological systems are exposed due to heavy metal contamination are so much alarming. Thus, the removal of such pollutants from water resources and wastewater is essential for human health and the environment protection [1,2]. Cadmium is a toxic and nondegradable pollutant present in aquatic systems as a result of anthropogenic activities. Consequently, its concentration can reach up to grams per liter levels exceeding its 10–100 mg L^{-1} fresh water content [3], causing serious threat to human health and biota. Cadmium is considered as a human carcinogen and teratogenesis impacting lungs, kidneys, liver and reproductive organs [4,5]. According to the World Health Organization (WHO) guidelines, the permissible concentration for cadmium in drinking water is 0.003 mg.L^{-1} [6].

Adsorption is a low-cost, highly efficient and easy to apply procedure for contaminants elimination. Low-cost and abundance of naturally available sorbents such as clays, zeolites, biomass, activated carbon, dried plant parts, saw dust, biopolymers, metal oxides and fly ash have been employed for cadmium removal [7–10]. Recently, nanomaterials have been used for the removal of heavy metal ions. For instance, Arce et al. [11] used modified silica nanoparticles to remove Cd(II) and Pb(II) from aqueous solutions, while green

* Corresponding author.

manufactured $CuFe_2O_4$ and nano zerovalent iron particles [5], γ-Fe_2O_3 nanotubes [12] and carbon nanotubes [13] were utilized to remove Cd(II) from aqueous solutions with varying adsorption capacities.

It is well known that ZnO is an environmental friendly material, and its surface has many functional groups, such as hydroxyl groups, which can be active sites for adsorption and uptake of positively charged ions [14–16]. It finds numerous applications such as catalysts [17,18], gas sensors [19], solar cells [20], and organic and inorganic pollutants removal [21].

In this work, ZnO nanoparticles were employed in Cd(II) ions removal from aqueous solutions. The kinetics and equilibrium of the adsorption process were investigated. The thermodynamic parameters were calculated to understand the nature of the ion adsorption onto the nanoparticles. A mechanism for the adsorption was proposed as well.

2. Material and methods

2.1. Material

The zinc oxide (ZnO) nanopowder was prepared via a sol-gel method under supercritical conditions of ethyl alcohol (EtOH) based on Omri et al. [22,23] protocol. The structural characteristics of the so-produced nanopowder pores were determined from the adsorption-desorption isotherms of N_2 at 77 K, through an apparatus ASAP 2020 (Micromeritics). The surface area of ZnO powder was calculated from the BET (Brunauer–Emmett–Teller) equation. The volume of micropores and the surface area were calculated from the t-plot method of Lippens and de Boer [24].

A stock solutions (1,000 mg.L^{-1}) of Cd(II) were prepared by dissolving cadmium nitrate ($Cd(NO_3)_2$ in distilled water. Experimental solutions at the desired concentrations were then obtained by successive dilutions. The pH was adjusted using HNO_3 and NaOH solutions. All the reagents were of analytical grade or highest purity available, and used without further purification.

2.2. Methods

Experiments were carried out in batch mode by adding 10 mg of adsorbent to 25 ml of a known Cd(II) solution concentration in a 50-ml Erlenmeyer flask. Adsorption studies were conducted at fixed pH value (7.0) and initial metal ion concentrations (20–140 mg.L^{-1}) to obtain equilibrium isotherms. Several flasks were placed on a multiposition magnetic stirrer and individually stirred at 500 rpm. After 12 h of contact, 15 ml of suspension was sampled from each flask, centrifuged (centrifuge, Hettich Zentrifugen EBA 20) and then passed through filter paper. Residual cadmium metal ion concentration in filtrate was measured with an inductively coupled plasma apparatus (Genius, ICP-EOS, Germany).

The amount of adsorbed metal ions was calculated according to the following equation:

$$q_t = \frac{V(C_0 - C_t)}{m} \quad (1)$$

where q_t (in mg.g^{-1}) is the amount of solute adsorbed per unit mass of adsorbent at time t (min); V is the solution volume (L); C_0 is the initial concentration metal ion (mg.L^{-1}); C_t (mg.L^{-1}) is the concentration of metal ion in solution at time t (minutes); and m the mass of ZnO adsorbent (g). The amount adsorbed (mg metal ion/g adsorbent) at equilibrium q_e was calculated using a similar equation:

$$q_e = \frac{V(C_0 - C_e)}{m} \quad (2)$$

where C_e is the liquid-phase concentration of Cd(II) at equilibrium time.

The equilibrium established between adsorbed and unadsorbed components in solution can be represented by adsorption isotherms. The most widely used isotherm equations for equilibrium data modeling are the Langmuir (Eq. (3)) and the empirical Freundlich (Eq. (4)) models:

$$\frac{C_e}{q_e} = \frac{1}{q_m} C_e + \frac{1}{q_m . K_L} \quad \text{linear form of Langmuir equation} \quad (3)$$

$$\ln q_e = \frac{1}{n} \ln C_e + \ln K_F \quad \text{linear form of Freundlich equation} \quad (4)$$

where q_m is the solid-phase concentration corresponding to the complete monolayer coverage of adsorption sites [25], and K_L is a constant related to the free energy of adsorption. Values of q_m and K_L can be graphically determined from the linear form of the Langmuir model (Eq. (3) as the slope is $1/q_m$ and the intercept $1/(q_m . K_L)$. The constants k and n of the Freundlich model are, respectively, obtained from the intercept and the slope of the linear plot of $\ln q_e$ vs. $\ln C_e$ (Eq. (4)). The constants K_F and n of the Freundlich model can be related to the strength of adsorptive bond and the bond distribution, respectively [26].

In fact, the kinetic study is generally done using various models, but in this work the pseudo-first- and pseudo-second-order kinetics models were tested to predict the adsorption data of Cd(II) as a function of time. According to Gupta et al. [27], the first-order model can be expressed as follows:

$$\ln(q_e - q_t) = \ln(q_e) - k_1 . t \quad (5)$$

where k_1 (min^{-1}) is the adsorption rate constant; k_1 and q_e can be determined from the slope and intercept of $\ln(q_e - q_t)$ vs. t plots, respectively. According to Ho and McKay [28], sorption kinetics can be represented by a pseudo-second-order model that leads to the following equation:

$$\frac{t}{q_t} = \frac{1}{k_2 . q_e^2} + \frac{t}{q_e} \quad (6)$$

where k_2 is the pseudo-second-order rate constant (g.mg^{-1}·min^{-1}). An adequate pseudo-second-order kinetic model should show a linear plot of t/q_t vs. t. The value of q_e can be easily deduced from the slope of the plot of t/q_t vs. t. Once q_e is identified, the value of k_2 can be obtained.

The thermodynamic properties: enthalpy change ($\Delta H°$), free energy change ($\Delta G°$) and entropy change ($\Delta S°$) for the adsorption of Cd(II) by the adsorbent are calculated from the following set of equations:

$$\Delta G^0 = -R.T.\ln K \quad (7)$$

$$\Delta S^{\circ} = \frac{\Delta H^{0} - \Delta G^{0}}{T} \quad (8)$$

The thermodynamic equilibrium constant, or the thermodynamic distribution coefficient *K*, is defined by Tu et al. [1] as follows:

$$K = \frac{a_s}{a_e} = \frac{\nu_s C_s}{\nu_e C_e} \quad (9)$$

where a_s and a_e are the activities of adsorbed and residual Cd(II) in solution at equilibrium, respectively; v_S and v_e show the activity coefficients of the adsorbed Cd(II) and the residual Cd(II) in solution, respectively; C_e and C_s are Cd(II) concentrations in solution at equilibrium and at the surface (mmol.g^{-1}) of adsorbent, respectively. As the metal ion concentration in the solution almost diminishes to zero; k can be obtained by drawing ln(C_s/C_e) vs. C_s and extrapolating C_s to zero [1,25]. The intercept at the vertical axis provides the values of *k*.

3. Result and discussion

3.1. Nitrogen isotherm

The isotherm shape provides information on pore size, which is usually categorized as micropore, mesopore, or macropore. As shown in Fig. 1, the adsorption-desorption isotherm of N_2 at 77 K is clearly of type II, according to the International Union of Pure and Applied Chemistry (IUPAC) classification of sorption isotherms [29], formerly designated as Brunauer's classification. The isotherm is a type H4 hysteresis loop, characteristic of aggregated particles with nonporous or macroporous adsorbents and unrestricted monolayer-multilayer adsorption.

The hysteresis, at $P/P_0 \approx 0.4$–1, is attributed to capillary condensation in mesopores corresponding in the voids between the ZnO powder particles [30]. The point at the beginning of the linear section of the isotherm, is often taken to indicate the stage at which monolayer coverage is complete and multilayer adsorption is about to begin [31]. The specific surface area of 8.25 m^2.g^{-1}, determined by the conventional BET method, is a characteristic of a material with low porosity or a crystallized material [32,33], with porous volume of about 0.072 cm^3.g^{-1}. The mean pore size determined from BET surface area, and the pore volume in the approximation of cylindrical pores is about 46.5 nm indicating a mesoporous nanopowder.

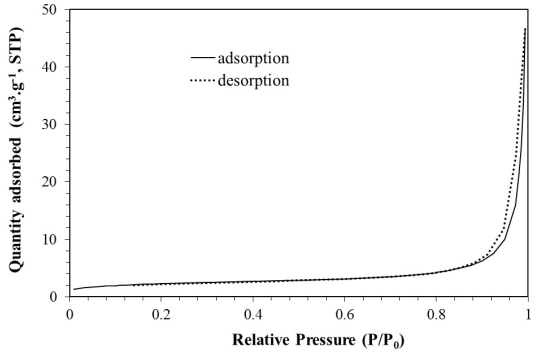

Fig. 1. Adsorption-desorption isotherms of N_2 at 77 K of zinc oxide.

3.2. The pH effect

The effect of pH on the initial concentration of Cd(II) ions was investigated in a pH range of 3–10 and 50 mg L^{-1} without ZnO nanoparticles, to determine the pH at which the Cd(II) ions start to precipitate. Fig. 2(a) clearly shows that the Cd(II) ion concentration in the solution is constant up to pH ≈ 7.0 and then drastically drops beyond that pH value. This finding may indicate the precipitation of the metal ions as hydroxides at higher pH. Accordingly, the pH value of 7.0, which is lower the critical pH of Cd(II) precipitation of 9.03 [34], was chosen to carry out all further investigations. The capacity of ZnO nanoparticles to eliminate the Cd(II) ion at different pH values is shown in Fig. 2(b). It can be seen that at lower pH the removal efficiency is very low. As has been previously reported [35], at low pH, the protons (H^+) in the solution compete with the Cd(II) ions for the adsorption sites, thus lowering the removal efficiency. On the other hand at almost neutral pH (6–7), this competition becomes weaker leading to enhanced removal efficiency. Conversely, at higher pH the probable formation of $Cd(OH)^+$ and/or $Cd(OH)_2$ [36] suppresses the removal efficiency. This is manifested by the

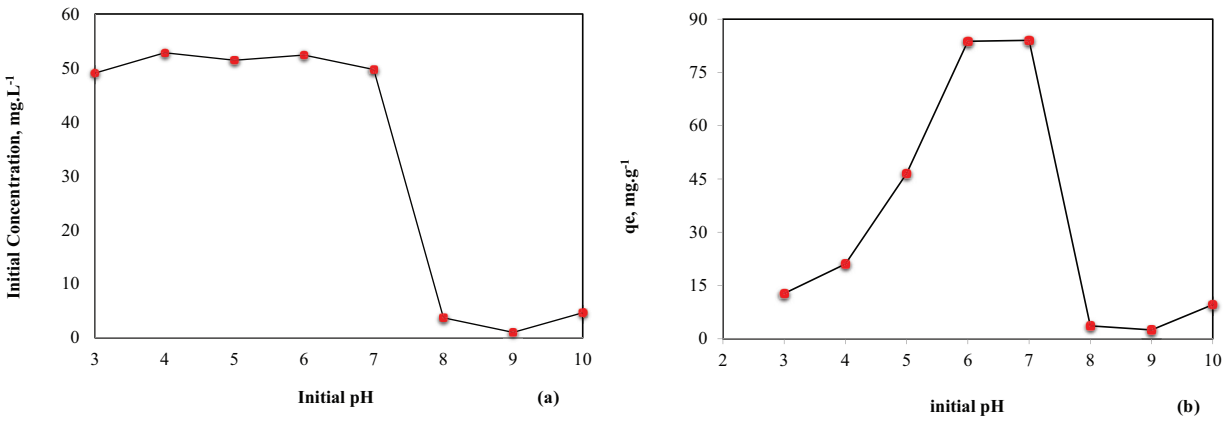

Fig. 2. The effect of pH values on: (a) the initial concentration and (b) the amount (q_e) of Cd(II) metal ions removal.

drastic drop of removal efficiency at pH value greater than 7.0 as shown in Fig. 2(b).

3.3. Heavy metals ions adsorption study

3.3.1. Kinetic study

The evolution of the sorption data of Cd(II) as a function of time is illustrated by Fig. 3 for the nanopowder at 298 K. It appears from Fig. 3 that there is a rapid initial rise of the adsorption capacities q_t. After 120 min, the Cd(II) adsorption did not change with the contact time. Thus, 120 min was considered as the appropriate time to attain equilibrium. The time required to reach equilibrium is considerably long compared with that reported by Tu et al. [1], where the maximum adsorption capacity of Cd(II) was found to be 17.54 mg g^{-1} at a contact time of 30 min. On the other hand, a time of 12 h was reported [2] for the adsorption of Cd(II) onto nano zerovalent iron particles when the initial concentration of the ions was 112.5 mg L^{-1}. The dependence of equilibrium time on initial concentrations was indicted by Rao and Khan [37], who reported 10, 50 and 60 min for an initial Cd(II) concentrations of 15, 25 and 50 mg L^{-1}, respectively.

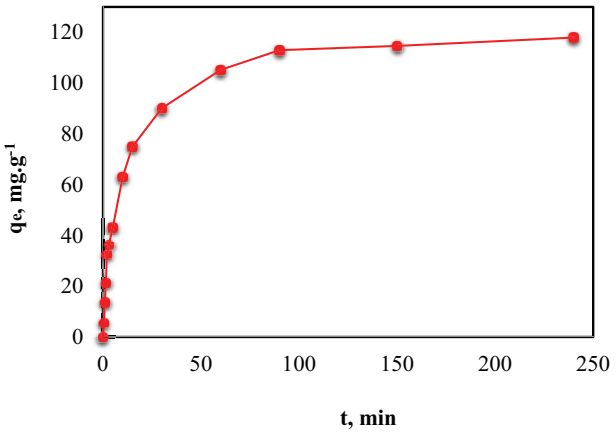

Fig. 3. Plot of the adsorption capacity of Cd(II) on ZnO nanopowder as a function of time.

In Fig. 4(a) a plot of $\ln(q_e - q_t)$ vs. t is represented. The plot shows linearity with regression coefficient $r^2 = 0.9071$. While the plot of t/q_t vs. t given in Fig. 4(b), assigned to the pseudo-second-order model, shows a better fitting for the data ($r^2 = 0.9998$). Concurrently, the calculated q_m value is in agreement with that obtained experimentally (Table 1). These results emphasize a better fitting of the pseudo-second-order kinetic model for the Cd(II) adsorption on ZnO nanoparticles. Similar results were reported where better fitting of the pseudo-second-order model compared with the pseudo-first-order model for Cd(II) adsorption on different adsorbents [2,38–41] was achieved.

3.3.2. Equilibrium study

Adsorption isotherms help to explain the adsorption process at equilibrium conditions. From such isotherms, an adsorbent capacity can be determined, enabling us to understand the proper adsorption mechanism. The most popular adsorption isotherms commissioned to fit these experimental data are the Freundlich and Langmuir models.

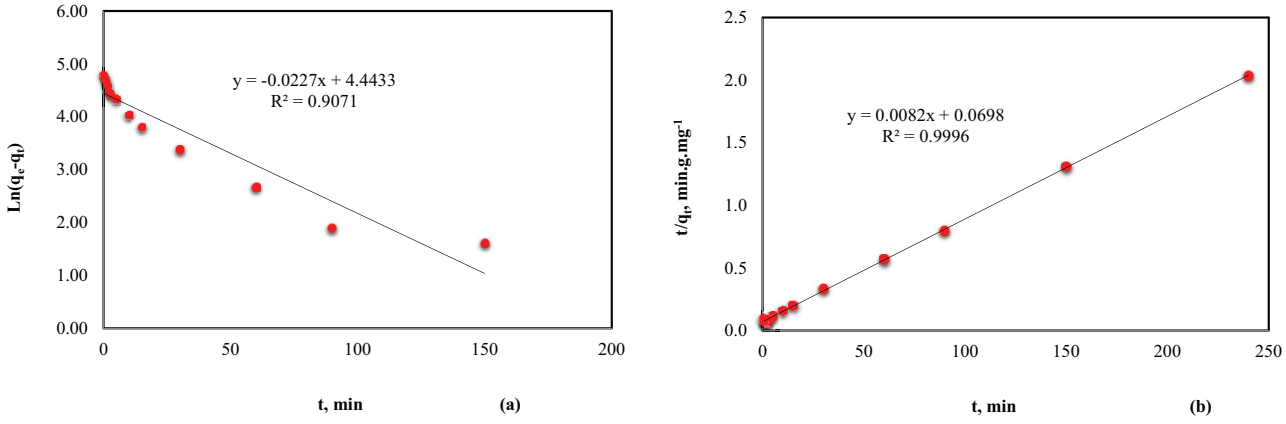

Fig. 4. Kinetics of Cd(II) adsorption onto ZnO: (a) pseudo-first-order plot and (b) pseudo-second-order plot. Conditions: 300 K, pH = 7, 0.12 g ZnO in 0.2 L of solution 95 mg.L^{-1}.

Table 1
Rate adsorption constants for the adsorption of Cd(II) by the adsorbent

$q_{m(exp)}$ [a] (mg.g^{-1})	$t^{1/2}$ (min)	First-order			Second-order		
		$k_1 \times 10^3$ (min^{-1})	$q_{m(cal)}$ [b] (mg.g^{-1})	r^2	$k_2 \times 10^3$ (g.mg^{-1}.min^{-1})	$q_{m(cal)}$ [b] (mg.g^{-1})	r^2
119.75	8.5	2.27	85.06	0.9071	9.6	121.95	0.9996

Figs. 5(a) and (b) reveals the adsorption isotherms of Cd(II) ions on ZnO nanoparticles at various temperatures (300, 313 and 328 K) and 7.0 pH. The batch experiments data were fitted to the isotherm models of the Langmuir and Freundlich using the least squares method. The linearized Langmuir and Freundlich isotherms of Cd(II) (Figs. 5(a) and (b)) in solutions are drawn, and the estimated model respective parameters (q_m, K_L, K_F and n) with correlation coefficient (r^2) are gathered in Table 2.

Considering the high values of the regression coefficient ($r^2 \approx 1.0$) as shown in this table, it is clear that Langmuir model exhibits a better fitting for the Cd(II) adsorption equilibrium data. The Cd(II) adsorption capacity and removal efficiency increased with the rise in temperature; the q_m increased from 178.6 to 217.4 mg.g^{-1} when temperature changed from 300 to 328 K suggesting the endothermic nature of the adsorption.

The essential features of the Langmuir isotherm may be expressed in terms of equilibrium parameter R_L, which is a dimensionless constant referred to as separation factor or equilibrium parameter [42]:

$$R_L = \frac{1}{1 + b.C_0} \tag{10}$$

where C_0 is the initial concentration; b is the constant related to the energy of adsorption (Langmuir constant). R_L value indicates the adsorption nature as irreversible if $R_L = 0$, favourable if $0 < R_L < 1$, linear if $R_L = 1$ and unfavorable if $R_L > 1$.

From this research finding, the maximum monolayer coverage capacity (Q_o) from Langmuir isotherm model was found to be 217.4 mg.g^{-1}, and R_L (the separation factor) is 0.92 indicating that the equilibrium sorption was favorable and the r^2 value of about 0.9950 proving that the sorption data fitted well to Langmuir isotherm model.

The cadmium adsorption capacity on ZnO nanoparticles at room temperature (297 K) was 217.4 mg.g^{-1} (Table 2). This finding makes it a superior adsorbents compared with those reported in the literature: hematite (4.94 mg.g^{-1}) [10], bone char (64.1 mg.g^{-1}) [43], orange waste (48.3 mg.g^{-1}) [38], wheat stem (11.6 mg.g^{-1}) [44], activated carbon (3.37 mg.g^{-1}) [45], chitin (14.7 mg.g^{-1}) [7], activated sludge (204.1 mg.g^{-1}) [46], and biogenic Mn oxides (229.3 mg.g^{-1}) [47].

3.3.3. Thermodynamic study

The effect of temperature was investigated for Cd(II) adsorption tests at 300, 313 and 328 K and pH 7.0. The amount of Cd(II) removed by the adsorbents rises with temperature as shown in the Langmuir isotherm plots of Fig. 6.

Considering the results obtained in section 3.3.2 concerning equilibrium studies, only Langmuir model is applied to the experimental adsorption data. Langmuir equation constants are listed in Table 2. The thermodynamic distribution coefficient K values for the different temperatures were obtained from Fig. 7 using Eq. (9). The value of enthalpy change ($\Delta H°$) was determined from the slope of the linear curve of ln(K) vs. the reciprocal temperature (1/T) (Fig. 8). The free energy change ($\Delta G°$) and entropy change ($\Delta S°$) values were calculated from Eqs. (5) and (6). Thermodynamic parameters are gathered in Table 3. The positive value of D$H°$ indicates the endothermic nature of the adsorption process.

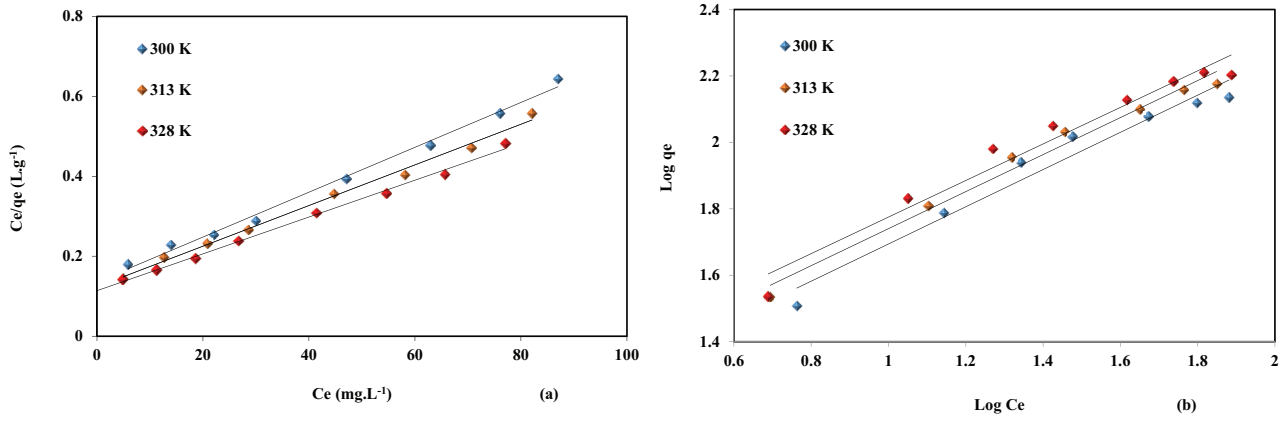

Fig. 5. Linearized adsorption equilibrium isotherms of Cd(II) at different temperatures by adsorbent nanopowder: (a) Langmuir linear equation and (b) Freundlich linear equation.

Table 2
Equilibrium constants for the Cd(II) ions removal

T (K)	q_m (mg.g^{-1})	Langmuir constants			Freundlich constants		
		K_L (l.mg^{-1})	R_L	r^2	n	k_f	r^2
300	178.6	7.6	0.9097	0.9938	1.785	13.61	0.9593
313	196.1	6.3	0.9241	0.9946	1.795	15.25	0.9791
328	217.4	5.2	0.9360	0.9956	1.818	16.79	0.9626

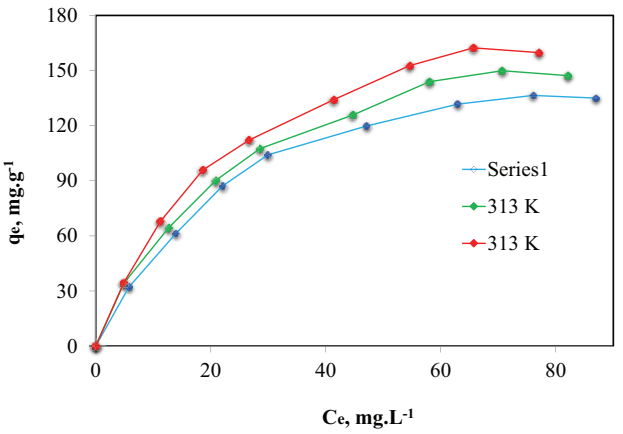

Fig. 6. Langmuir isotherms for the adsorption of Cd(II) onto ZnO nanopowder at different temperatures.

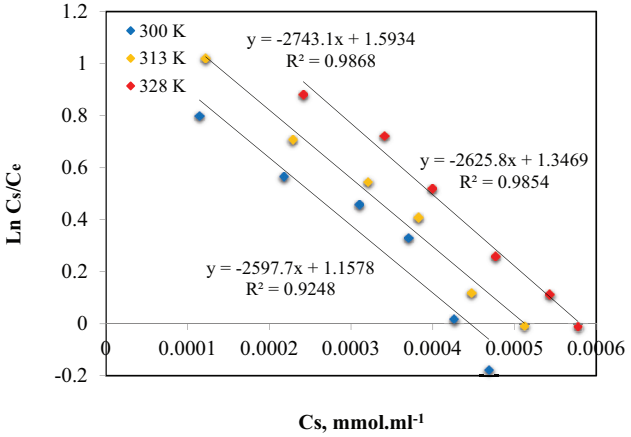

Fig. 7. Plots $\ln(C_s/C_e)$ vs C_s at different temperatures.

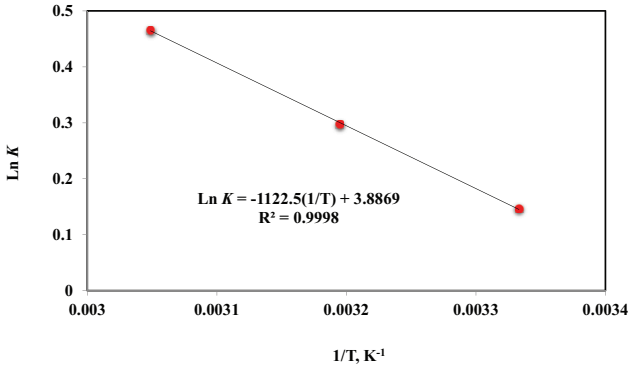

Fig. 8. Plot of ln*K* vs. the reciprocal temperature for cadmium ion adsorption by ZnO nanopowder.

This is clearly evidenced by the enhancement of Cd(II) adsorption at higher temperatures. Also, the $\Delta H°$ value suggests an electrostatic attraction between Cd(II) ions and ZnO nanopowder in a physical adsorption process. Moreover, the positive value of $\Delta H°$ may be attributed to removal of water molecules from the hydrated metal ions as well as solid–solution interface [33]. Thus, the energy released when the ions are attached to the adsorbent surface will be used up by this dehydration process resulting in an overall endothermic sorption [48]. The positive values of D*S*° suggest an increased randomness at the solid-solution interface.

Table 3
Thermodynamic parameters for Cd(II) adsorption

Temperature (K)	*K*	$\Delta G°$ (kJ.mol^{-1})	$\Delta S°$ (kJ.mol^{-1}.K^{-1})	$\Delta H°$ (kJ.mol^{-1})	r^2
298	1.1578	–0.365	0.0323	9.334	0.9998
306	1.3469	–0.775	0.0323		
313	1.5934	–1.271	0.0323		

The negative values of the free energy change (D*G*°) confirm the spontaneous nature of adsorption. The change of the standard free energy decreases with increasing temperatures regardless of the nature of adsorbent. This indicates that a better adsorption is actually obtained at higher temperatures.

3.3.4. Mechanism of adsorption

Mosayebi and Azizian [49] proposed a mechanism for the removal of Cu(II) by ZnO and $Zn(OH)_2$ based on the effect of the solutions pH. As the pH is close to the pH_{pzc} a decrease of the repulsive interaction between the adsorbent surface and adsorbate results in an increase in positive ions removal. The same argument can be applied to the Cd(II) ions and a complex formation [50] which can be suggested as follows:

$$\text{~ZnOH} + Cd^{+2} \leftrightarrow \text{~ZnOCd}^{+} + H^{+}$$

The equilibrium will be shifted to the right as the pH is increased.

The uptake of cadmium ions can be controlled either by a mass transfer in the boundary film of liquid or by an intra-particular mass transfer. The external mass transfer coefficient, β_L (m.s^{-1}) of Cd(II) in the boundary film, may be evaluated by using the formula [51,52]:

$$\ln\left(\frac{C_t}{C_0}-\frac{1}{1+m.K_a}\right)=\ln\left(\frac{m.K_a}{1+m.K_a}\right)-\left(\frac{1+m.K_a}{m.K_a}\right).\beta_L.S_S.t \quad (11)$$

where C_t and C_0 (both in mg.L^{-1}) are the respective concentrations of the metal ion at time *t* and zero, K_a (L.g^{-1}) is a constant defined as the product of the Langmuir constants: $K_a = Q_0.b$; *m*(g) is the adsorbent mass, and S_S is the adsorbent surface area (m^2.g^{-1}). A straight line in $\ln[(C_t/C_0 - 1/(1 + m.K_a)]$ vs. *t* plot is required to prove the reliability of model.

The adsorbed species may also be transported from the solution bulk to the solid phase through intra-particle diffusion/transport process. The intra-particular diffusion is the limiting step in many adsorption processes. The possibility of intra-particular diffusion is explored by using the Weber and Morris diffusion mode [53,54]:

$$q_t = k_{dif}.t^{1/2} + C \quad (12)$$

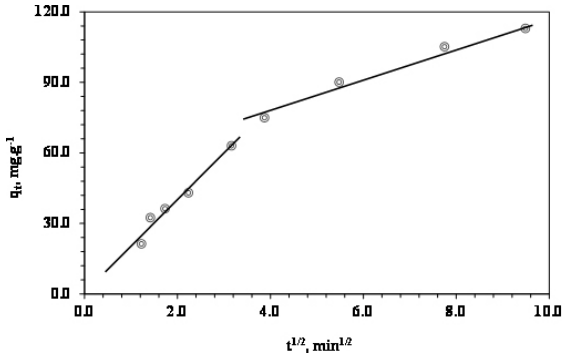

Fig. 9. q_t vs. $t^{1/2}$ plot for the intraparticle diffusion.

Table 4
Kinetic parameters for the Cd(II) ions adsorption onto ZnO nanoparticles based on the intraparticle diffusion model

Intraparticle diffusion equation Parameters					
k_{dif1}, mg/g.min$^{1/2}$	C	r^2	k_{dif2}, mg/g.min$^{1/2}$	C	r^2
19.023	1.9559	0.9834	6.7368	51.04	0.9795

where C is the intercept, and k_{dif} is the intra-particle diffusion rate constant. The k_{dif} values for the tested adsorbent are calculated from the slopes of the plots (Fig. 9) and reported in Table 5. The validity of these models is thereafter discussed.

The mass transfer rate model lying on a linear relationship between $\ln[(C_t/C_0 - 1/(1 + m.ka)]$ and t did not provide a linear plot, demonstrating the invalidity of this model. The values of regression coefficient calculated from Eq. (11) for ZnO nanopowder is about 0.86. This means that the uptake of cadmium ions at the tested adsorbent sites is not governed by liquid phase mass transfer rate. Instead, the uptake of Cd(II) at the surface of the adsorbent may be governed by the intra-particle diffusion kinetic model, since the values of q_t are found to be linearly correlated with $t^{1/2}$ values. Besides, the regression coefficient values are equal to 0.98 indicating the applicability of this model. The intra-particle diffusion plots are shown in Fig. 9. Main parameters of this model are determined and gathered in Table 4. The values of intercept (i.e., C, Table 4) give an idea about the boundary layer thickness. The larger intercept, the greater is the boundary layer effect.

The intraparticle diffusion plot of q_t vs. $t^{1/2}$ (Fig. 9) shows two stages sorption, i.e., multilinear [55]. The first stage is a sharp one that may have resulted from the diffusion of Cd(II) through the solution to the external surface of nanoparticles then to the surface through the boundary layer. Meanwhile, the second stage may indicate the final equilibrium where the intraparticle diffusion starts to slow down as a result of the lower concentration gradient of Cd(II) ions.

From the tabulated results (Table 4), it can be seen that the diffusion rate has decreased by increasing the contact time due to the smaller pores accessible for diffusion as the Cd(II) ions previously diffuse into the inner structure of nanoparticles in the first stage. This is evidenced by the smaller value of rate parameters k_{dif2} compared k_{dif1}. Also, the constant related to the boundary layer thickness (C) is larger in the second stage showing greater boundary layer effect [56].

Table 5
A comparison of ZnO adsorption capacity with some nanoadsorbents for cadmium (II)

Adsorbent	q_e (mg.g^{-1})	T (K)	Ref.
Carbon nanotubes	11.00	298	[57]
Nano NH_2-MCM-41	18.25	298	[58]
$CuFe_2O_4$ nanoparticles	17.54	298	[1]
Magnetic graphene oxide	91.29	298	[59]
Milled goethite	125	298	[40]
Milled goethite	167	328	[40]
Ni (15 wt%)-doped α-Fe_2O_3	-90.91	328	[41]
ZnO	179	298	Present study
ZnO	217	328	Present study

Table 6
Regeneration data for ZnO nanoparticles

Cycle	1	2	3
% recovery	90	85	79

4. Comparison of Cd(II) adsorption capacity with different adsorbents

The adsorption capacity of ZnO nanoparticles for the Cd(II) ions removal was contrasted with that of some nanoadsorbents, reported in literatures as listed in Table 5. The adsorbent used in this work exhibited higher adsorption capacity than other nanostructure adsorbents, indicating that the ZnO is a promising adsorbent of Cd(II) ions from water and wastewater.

5. Regeneration of catalyst

To investigate the reusability of the nanoparticles, the catalyst was recovered by filtration from the reaction mixture after washing with ethyl acetate, methanol and distilled water. After drying the experiments were done by adding 50 ml of 100 mg.L^{-1} Cd(II) to 10 mg of ZnO under the previous experimental conditions for 3 cycles. Table 6 depicts the percentage recovery, indication the efficiency of the ZnO nanaoparticles without significant loss in its removal capacity.

6. Conclusion

A suitable indigenous nanomaterial elaborated by a modified sol-gel method has been identified as an effective adsorbent for the uptake of cadmium metal ions from aqueous solutions. The equilibrium data of adsorption are in good agreement with the Langmuir's model. Furthermore, it was found that a second-order kinetics rate model well mimics the kinetic data for the cadmium ions removal. Besides, temperature is a determinant factor for the Cd(II) ions removal. Increasing temperature not only enhances the rate of adsorption, but also its extent. This finding can be explained by the positive value found for the enthalpy change of the adsorption reaction. Whereas, the positive values of the entropy suggest an increase of randomness at the solid–solution interface during the heavy metal

ions adsorption. The negative values of the free energy with low enthalpy value at different temperatures suggest a spontaneous physical adsorption process. The adsorption mechanism is controlled by diffusion as well as boundary layer effect.

Acknowledgment

The authors would like to thank the National Plan, for Sciences, Technology and Innovation (MAARIFAH) – King Abdulaziz City for Sciences & Technology, Kingdom of Saudi Arabia.

References

[1] Y.J. Tu, C.F. You, C.K. Chang, Kinetics and thermodynamics of adsorption for Cd on green manufactured nanoparticles, J. Hazard. Mater., 235–236 (2012) 116–122.
[2] H.K. Boparai, M. Joseph, D.M. O'Carroll, Kinetics and thermodynamics of cadmium ion removal by adsorption onto nano zerovalent iron particles, J. Hazard. Mater., 186 (2011) 458–465.
[3] G.F. Nordberg, B.A. Fowler, M. Nordberg, L.T. Friberg, Handbook on the Toxicology of Metals, 3rd ed., Academic Press, Elsevier, California, 2007.
[4] H. Wang, Y.F. Jia, S.F. Wang, H.J. Zhu, X. Wu, Bioavailability of cadmium adsorbed on various oxides minerals to wetland plant species Phragmites australis, J. Hazard. Mater., 167 (2009) 641–646.
[5] J.L. Pan, J.A. Plant, N. Voulvoulis, C.J. Oates, C. Ihlenfeld, Cadmium levels in Europe: implications for human health, Environ. Geochem. Health, 32 (2010) 1–12.
[6] WHO, Guidelines for Drinking Water Quality: Recommendations, Vol. 1, 3rd ed., World Health Organization, Geneva, 2008.
[7] B. Benguella, H. Benaissa, Cadmium removal from aqueous solutions by chitin: kinetic and equilibrium studies, Water Res., 36 (2002) 2463–2474.
[8] R. Cortes-Martinez, V. Martinez-Miranda, M. Solache-Rios, I. Garcia-Sosa, Evaluation of natural and surfactant-modified zeolites in the removal of cadmium from aqueous solutions, Sep. Sci. Technol., 39 (2004) 2711–2730.
[9] Z.Z. Li, T. Katsumi, S. Imaizumi, X.W. Tang, T. Inui, Cd(II) adsorption on various adsorbents obtained from charred biomaterials, J. Hazard. Mater., 183 (2010) 410–420.
[10] D.B. Singh, D.C. Rupainwar, G. Prasad, K.C. Jayaprakas, Studies on the Cd(II) removal from water by adsorption, J. Hazard. Mater., 60 (1998) 29–40.
[11] V.B. Arce, R.M. Gargarello, F. Ortega, V. Romañano, M. Mizrahi, J.M. Ramallo-López, C.J. Cobos, C. Airoldi, C. Bernardelli, E.R. Donati, D.O. Mártire, EXAFS and DFT study of the cadmium and lead adsorption on modified silica nanoparticles, Spectrochim. Acta, Part A, 151 (2015) 156–163.
[12] A. Roy, J. Bhattacharya, A binary and ternary adsorption study of wastewater Cd(II), Ni(II) and Co(II) by γ-Fe_2O_3 nanotubes, Sep. Purif. Technol., 115 (2013) 172–179.
[13] D.K. Venkatramana, J.S. Yu, K. Seshaiah, Silver nanoparticles deposited multiwalled carbon nanotubes for removal of Cu(II) and Cd(II) from water: surface, kinetic, equilibrium and thermal adsorption properties, Chem. Eng. J., 223 (2013) 806–815.
[14] X. Wang, W. Cai, Y. Lin, G. Wang, C. Ling, Mass production of micro/nanostructured porous ZnO plates and their strong structurally enhanced and selective adsorption performance for environmental remediation, J. Mater. Chem., 20 (2010) 8582–8590.
[15] Y. Kikuchi, Q.R. Qian, M. Machida, H. Tatsumoto, Effect of ZnO loading to activated carbon on Pb(II) adsorption from aqueous solution, Carbon, 44 (2006) 195–202.
[16] F. Joodaki. S. Azizian, S. Sobhanardakani, Synthesis of nanostructured ZnO loaded on carbon cloth as high potential adsorbent for copper ion, Desal. Wat. Treat., 55 (2015) 596–603.
[17] Y. Sun, L. Wang, X. Yu, K. Chen, Facile synthesis of flower-like 3D ZnO superstructures *via* solution route, CrystEngComm, 14 (2012) 3199–3204.
[18] H.B. Zeng, W.P. Cai, P.S. Liu, X.X. Xu, H.J. Zhou, C. Klingshirn, H. Kalt, ZnO-based hollow nanoparticles by selective etching: elimination and reconstruction of metal−semiconductor interface, improvement of blue emission and photocatalysis, ACS Nano, 2 (2008) 1661–1670.
[19] Z.H. Jing, J.H. Zhan, Fabrication and gas-sensing properties of porous ZnO nanoplates, Adv. Mater., 20 (2008) 4547–4551.
[20] T.P. Chou, Q.F. Zhang, G.E. Fryxell, G.Z. Cao, Hierarchically structured ZnO film for dye-sensitized solar cells with enhanced energy conversion efficiency, Adv. Mater., 19 (2007) 2588–2592.
[21] D. Mohan, A. Sarswat, Y.S. Ok, C.U. Pittman Jr., Organic and inorganic contaminants removal from water with biochar, a renewable, low cost and sustainable adsorbent – a critical review, Bioresour. Technol., 160 (2014) 191–202.
[22] K. Omri, I. Najeh, R. Dhahri, J. El Ghoul, L. El Mir, Effects of temperature on the optical and electrical properties of ZnO nanoparticles synthesized by sol–gel method, Microelectron. Eng., 128 (2014) 53–58.
[23] K. Omri, J. El Ghoul, O.M. Lemine, M. Bououdina, B. Zhang, L. El Mir, Magnetic and optical properties of manganese doped ZnO nanoparticles synthesized by sol–gel technique, Superlattices Microstruct., 60 (2013) 139–147.
[24] B.C. Lippens, J.H. de Boer, Studies in pore systems in catalysts: V. The *t* method, J. Catal., 4 (1965) 319–323.
[25] N. Chiron, R. Guilet, E. Deydier, Adsorption of Cu(II) and Pb(II) onto a grafted silica: isotherms and kinetic models, Water Res., 37 (2003) 3079–3086.
[26] Y.H. Li, Z. Di, J. Ding, D. Wu, Z. Luan, Y. Zhu, Adsorption thermodynamic, kinetic and desorption studies of Pb^{2+} on carbon nanotubes, Water Res., 39 (2005) 605–609.
[27] V.K. Gupta, S. Sharma, I.S. Yadau, D. Mohan, Utilization of bagasse fly ash generated in the sugar industry for the removal and recovery of phenol and *p*-nitrophenol from wastewater, J. Chem. Technol. Biotechnol., 71 (1998) 180–186.
[28] Y.S. Ho, G. McKay, Kinetic models for the sorption of dye from aqueous solution by wood, Process Saf. Environ. Prot., 76 (1998) 183–191.
[29] S.J. Gregg, K.S.W. Sing, Adsorption, Surface Area and Porosity, Academic Press, London, 1982, ISBN 0-12-300956-1.
[30] A.J. Lecloux, Catalysis Science and Technology, J.R. Anderson, M. Boudart, Eds., Springer, Berlin, Vol. 2, 1981, p. 171.
[31] K.S.W. Sing, D.H. Everett, R.A.W. Haul, L. Moscou, R.A. Pierotti, J. Rouquerol, T. Siemieniewska, Reporting physisorption data for gas/solid systems, Pure Appl. Chem., 57 (1985) 603—619.
[32] N. Azouaou, Z. Sadaoui, A. Djaafri, H. Mokaddem, Adsorption of cadmium from aqueous solution onto untreated coffee grounds: equilibrium, kinetics and thermodynamics, J. Hazard. Mater., 184 (2010) 126–134.
[33] P. Miretzky, C. Munoz, E. Cantoral-Uriza, Cd^{2+} adsorption on alkaline-pretreated diatomaceous earth: equilibrium and thermodynamic studies, Environ. Chem. Lett., 9 (2011) 55–63.
[34] L. Dong, A. Zhu, H. Ma, Y. Qiu, J. Zhao, Simultaneous adsorption of lead and cadmium on MnO_2-loaded resin, J. Environ. Sci., 22 (2010) 225–229.
[35] G. Yang, L. Tang, X. Lei, G. Zeng, Y. Cai, X. Wei, Y. Zhou, S. Li, Y. Fang, Y. Zhang, Cd(II) removal from aqueous solution by adsorption on α-ketoglutaric acid-modified magnetic chitosan, Appl. Surf. Sci., 292 (2014) 710–716.
[36] J. Duan, B. Su, Removal characteristics of Cd(II) from acidic aqueous solution by modified steel-making slag, Chem. Eng. J., 246 (2014) 160–167.
[37] R.A.K. Rao, M.A. Khan, Biosorption of bivalent metal ions from aqueous solution by an agricultural waste: kinetics, thermodynamics and environmental effects, Colloids Surf., A, 332 (2009) 121–128.
[38] A.B. Perez-Marin, V.M. Zapata, J.F. Ortuno, M. Aguilar, J. Saez, M. Llorens, Removal of cadmium from aqueous solutions by adsorption onto orange waste, J. Hazard. Mater., 139 (2007) 122–131.
[39] H. Javadian, F. Ghorbani, H. Tayebi, S.M.H. Asl, Study of the adsorption of Cd(II) from aqueous solution using zeolite-based geopolymer, synthesized from coal fly ash; kinetic, isotherm and thermodynamic studies, Arabian J. Chem., 8 (2015) 837–849.

[40] L. Khezami, M.O. M'hamed, O.M. Lemine, M. Bououdina, A. Bessadok-Jemai, Milled goethite nanocrystalline for selective and fast uptake of cadmium ions from aqueous solution, Desal. Wat. Treat., 57 (2016) 6531–6539.
[41] M.O. M'hamed, L. Khezami, A.G. Alshammari, S.M. Ould-Mame, I. Ghiloufi, O.M. Lemine, Removal of cadmium (II) ions from aqueous solution using Ni (15 wt.%)-doped α-Fe_2O_3 nanocrystals: equilibrium, thermodynamic, and kinetic studies, Water Sci. Technol., 72 (2015) 608–615.
[42] T.N. Webber, R.K. Chakravarti, Pore and solid diffusion models for fixed bed absorbers, AIChE J., 20 (1974) 228–238.
[43] C.W. Cheung, J.F. Porter, G. McKay, Sorption kinetic analysis for the removal of cadmium ions from effluents using bone char, Water Res., 35 (2001) 605–612.
[44] G.Q. Tan, D. Xiao, Adsorption of cadmium ion from aqueous solution by ground wheat stems, J. Hazard. Mater., 164 (2009) 1359–1363.
[45] H.K. An, B.Y. Park, D.S. Kim, Crab shell for the removal of heavy metals from aqueous solution, Water Res., 35 (2001) 3551–3556.
[46] R.D.C. Soltani, A.J. Jafari, Gh.S. Khorramabadi, Investigation of cadmium (II) ions biosorption onto pretreated dried activated sludge, Am. J. Environ. Sci., 5 (2009) 41–46.
[47] Y.T. Meng, Y.M. Zheng, L.M. Zhang, J.Z. He, Biogenic Mn oxides for effective adsorption of Cd from aquatic environment, Environ. Pollut., 157 (2009) 2577–2583.
[48] R.A. Shah, A.V. Shah, R.R. Singh, Sorption isotherms and kinetics of chromium uptake from wastewater using natural sorbent material, Int. J. Environ. Sci. Technol., 6 (2009) 77–90.
[49] E. Mosayebi, S. Azizian, Study of copper ion adsorption from aqueous solution with different nanostructured and microstructured zinc oxides and zinc hydroxide loaded on activated carbon cloth, J. Mol. Liq., 214 (2016) 384–389.
[50] C. Faur-Brasquet, Z. Reddad, K. Kadirvelu, P. Le Cloirec, Modeling the adsorption of metal ions (Cu^{+2}, Ni^{+2}, Pb^{+2}) onto ACCs using surface complexation model, Appl. Surf. Sci., 196 (2002) 356–365.
[51] V.P. Vinod, T.S. Anirudhan, Adsorption behaviour of basic dyes on the humic acid immobilized pillared clay, Water, Air, Soil Pollut., 150 (2003) 193–217.
[52] M.N. Sahmoune, N. Ouazene, Mass-transfer processes in the adsorption of cationic dye by sawdust, Environ. Prog. Sustain. Energ., 31 (2012) 597–603.
[53] B.H. Hameed, J.M. Salman, A.L. Ahmad, Adsorption isotherm and kinetic modeling of 2, 4-D pesticide on activated carbon derived from date stones, J. Hazard. Mater., 163 (2009) 121–126.
[54] A. El-Sikaily, A. El Nemr, A. Khaled, O. Abdelwehab, Removal of toxic chromium from wastewater using green alga *Ulva lactuca* and its activated carbon, J. Hazard. Mater., 148 (2007) 216–228.
[55] M. Yazdani, T. Tuutijärvi, A. Bhatnagar, R. Vahala, Adsorptive removal of arsenic (V) from aqueous phase by feldspars: kinetics, mechanism, and thermodynamic aspects of adsorption, J. Mol. Liq., 214 (2016) 149–156.
[56] N.B. Milosavljevi, M. Risti, A.A. Peric-Grujic, J.M. Filipovic, S.B. Strbac, Z.Lj. Rakocevic, M.T.K. Krusic, Removal of Cu^{2+} ions using hydrogels of chitosan, itaconic and methacrylic acid: FTIR, SEM/EDX, AFM, kinetic and equilibrium study, Colloids Surf., A, 388 (2011) 59–69.
[57] Y.H. Li, S.G. Wang, Z.K. Luan, J. Ding, C.L. Xu, D.H. Wu, Adsorption of cadmium (II) from aqueous solution by surface oxidized carbon nanotubes, Carbon, 41 (2003) 1057–1062.
[58] A. Heidari, H. Younesi, Z. Mehraban, Removal of Ni(II), Cd(II) and Pb(II) from a ternary aqueous solution by amino functionalized mesoporous and nano mesoporous silica, Chem. Eng. J., 153 (2009) 70–79.
[59] J.H. Deng, X.R. Zhang, G.M. Zeng, J.L. Gong, Q.Y. Niu, J. Liang, Simultaneous removal of Cd(II) and ionic dyes from aqueous solution using magnetic graphene oxide nanocomposite as an adsorbent, Chem. Eng. J., 226 (2013) 189–200.